

Microbiological Redox Potential Control to Improve the Efficiency of Chalcopyrite Bioleaching

Masaki, Yusei

Department of Earth Resources Engineering, Graduate School of Engineering, Kyushu University

Hirajima, Tsuyoshi

Department of Earth Resources Engineering, Graduate School of Engineering, Kyushu University

Sasaki, Keiko

Department of Earth Resources Engineering, Graduate School of Engineering, Kyushu University

Miki, Hajime

Department of Earth Resources Engineering, Graduate School of Engineering, Kyushu University

他

<https://hdl.handle.net/2324/4737396>

出版情報 : Geomicrobiology Journal. 35 (8), pp.648-656, 2018-04-03. Taylor and Francis
バージョン :
権利関係 :



Title: Microbiological Redox Potential Control to Improve the Efficiency of
Chalcopyrite Bioleaching

Yusei MASAKI, Tsuyoshi HIRAJIMA, Keiko SASAKI, Hajime MIKI, Naoko OKIBE*

Department of Earth Resources Engineering, Graduate School of Engineering, Kyushu
University, 744 Motoooka, Nishi-ku, Fukuoka 819-0395, Japan

*Corresponding author

Tel. and Fax: + 81 92 802 3312

E-mail address: okibe@mine.kyushu-u.ac.jp (Naoko Okibe)

RUNNING TITLE: Redox potential-controlled bioleaching

KEYWORDS: Chalcopyrite bioleaching; moderately thermophilic iron-oxidizers;
Solution redox potential (E_h); bioleaching kinetics

ABSTRACT: The effect of controlling the redox potential (E_h) on chalcopyrite bioleaching kinetics was studied as a new aspect of redox control during chalcopyrite bioleaching, and its mechanism was investigated by employing the “normalized” solution redox potential (E_{normal}) and the reaction kinetics model. Different E_h ranges were established by use of different acidophiles (*Sulfobacillus acidophilus* YTF1; *Sulfobacillus sibiricus* N1; *Acidimicrobium ferrooxidans* ICP; *Acidiplasma* sp. Fv-AP). Cu dissolution was very susceptible to real-time change in E_h during the reaction. It was found that efficiency of bioleaching of chalcopyrite can be effectively evaluated on the basis of E_{normal} , since it is normalized for real-time fluctuations of concentrations of major metal solutes during bioleaching. For steady Cu solubilization during bioleaching at a maximum rate, it was important to maintain a redox potential range of $0 \leq E_{\text{normal}} \leq 1$ (-0.35 mV optimal) at the mineral surface by employing a “weak” ion-oxidizer. This led to a copper recovery of > 75%. At higher E_{normal} levels ($E_{\text{normal}} > 1$ by “strong” microbial Fe^{2+} oxidation), Cu solubilization was slowed by diffusion through the product film at the mineral surface (< 50% Cu recovery) caused by low reactivity of the chalcopyrite and by secondary passivation of the chalcopyrite surface, mainly by jarosite.

Introduction

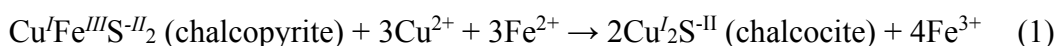
The demand for copper by a number of industrialized and economically emerging nations has been increasing steadily in the last decade. Even though chalcopyrite (CuFeS_2) ores are generally low-grade and highly refractory, they are an attractive source of copper because they constitute a significant component of porphyry copper deposits [approx. 70% of the world's copper reserves (Sillitoe, 2010)]. For this reason, a number of studies to improve the copper recovery by overcoming the very slow leaching/bioleaching kinetics are being undertaken, which depend on an improved understanding of the mechanism of chalcopyrite leaching.

Although a number of studies of chemical leaching of chalcopyrite using aqueous lixiviants (e.g., H_2SO_4 , HCl , HClO_4 with and without Fe^{3+}) have been done, no universal agreement on the nature of the chalcopyrite surface has been reached. The presence of elemental sulfur (S^0), disulfide (S_2^{2-}); polysulfide (S_n^{2-}) (metal deficient sulfide), Fe oxyhydroxide (jarosite-like species) have been proposed (Li et al. 2013). The leaching of metal sulfide ores was reported to be inhibited by formation of such passivating surface layers (e.g., Stott et al., 2000; Córdoba et al. 2009; Viramontes-Gamboa et al., 2010), but the nature of the surface layers is being debated. For instance, it was suggested that the presence of porous S^0 layers do not impede the leaching efficiencies significantly (Parker et al. 1981; Antonijevic et al. 1994; Córdoba et al. 2008, 2009). Such diversity in findings

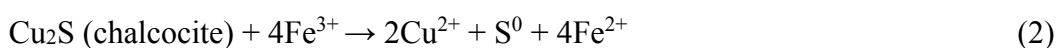
is often caused by differences in experimental conditions (e.g., pH, temperature, solute concentration (Li et al., 2013)).

Nonetheless, it is generally understood that one of the most important parameters governing bioleaching is the redox potential of the leaching solution (E_h): From a review of a number of electrochemical, chemical, and biological studies, Viramonetes-Gamboa et al. (2007; 2010) suggested that chalcopyrite leaching with ferric sulfate is in its active state at < 685 mV (SHE), regardless of impurities in the chalcopyrite, or the acidity or the temperature of the reaction. At 685-755 mV (SHE), chalcopyrite is in a bistable system (it could be passive or active depending on how it was brought to that potential). At > 755 mV (SHE), chalcopyrite leaching is in the passive state with a strong passivation effect.

Based on some electrochemical/chemical leaching studies, Hiroyoshi et al. (2000, 2001, 2004, 2008a, b) proposed a mechanism of chalcopyrite dissolution controlled by E_h levels. According to this mechanism, chalcopyrite leaching using ferric sulfate is enhanced by the presence of Fe^{2+} and Cu^{2+} , leading to the formation of intermediate chalcocite (Cu_2S) owing to the low E_h from the presence of Fe^{2+} (1). The oxidation of Cu_2S then yields Cu^{2+} (2):



$$\Delta G_1^0 = 35.0 \text{ kJ/mol}^{-1}$$



$$\Delta G_2^0 = - 81.1 \text{ kJ/mol}^{-1}$$

Copper recoveries are enhanced when $E_{\text{ox}} < E_h < E_c$ is satisfied (with an optimal potential of 630 mV (SHE); Hiroyoshi et al. 2000, 2008a), where;

E_c (“critical potential”) is the equilibrium redox potential of the formation of the

$$\text{intermediate chalcocite from chalcopyrite} \quad (E_c \text{ (V)} = E_c^0 + \frac{RT}{4F} \ln \frac{(a_{\text{Cu}^{2+}})^3}{a_{\text{Fe}^{2+}}}) \quad (3)$$

E_{ox} (“oxidation potential”) is the equilibrium redox potentials of the subsequent oxidation

$$\text{of chalcocite to Cu}^{2+} \quad (E_{\text{ox}} \text{ (V)} = E_{\text{ox}}^0 + \frac{RT}{4F} \ln (a_{\text{Cu}^{2+}})^2) \quad (4)$$

Since bioleaching is an economic approach for processing highly refractory chalcopyrite ores/concentrates, it is important to investigate the applicability of the above reactions (1) through (4) to this process. Previously, Gericke et al. (2010) and Ahmadi et al. (2010, 2011) reported on maximizing Cu extraction from chalcopyrite at 600-650 mV (SHE) by suppression of pyrite oxidation, thereby preventing jarosite formation. The aim of the present study was set to achieve a more comprehensive understanding of the mechanism of chalcopyrite leaching. Furthermore, microbiological E_h control instead of electrochemical/chemical control began to be studied as a new aspect of redox control of chalcopyrite bioleaching. Specific aims of the present study were (i) evaluation of the effect of “microbiological redox control” on chalcopyrite leaching through application of specific Fe-oxidizing microorganisms, and (ii) elucidation of the mechanism of chalcopyrite bioleaching in terms of reaction kinetics under specified low redox

potentials by considering the concept of E_{normal} .

Materials and Methods

Microorganisms

Five moderately thermophilic, acidophilic strains were used: (i) Fe-oxidizers; three bacterial species (*Sulfobacillus acidophilus* YTF1; *Sb. sibiricus* N1^T (DSM 17363); *Acidimicrobium ferrooxidans* ICP^T (DSM 10331)) and one archaeal species (*Acidiplasma* sp. Fv-Ap), (ii) S-oxidizer; *Acidithiobacillus (At.) caldus* KU^T (DSM 8584). The five strains were maintained and pre-grown aerobically at 45°C in heterotrophic basal salts (HBS) medium (Masaki et al. 2015; pH 1.5) supplemented with 0.01% (w v⁻¹) yeast extract (YE). Ten-millimolar Fe²⁺ (as FeSO₄·7H₂O) and 0.1% (w v⁻¹) S⁰ plus trace elements (TE; Masaki et al. 2016) were supplied to Fe-oxidizers and to S-oxidizing *At. caldus* KU, respectively. All pH adjustments in this work were made with H₂SO₄.

Mineral

Chalcopyrite concentrate (20-106 µm; JX Nippon Mining & Metals) was washed with 1 M HNO₃, deionized water and 100% ethanol before freeze-drying overnight. The elemental composition (Table I) was calculated from the ICP measurement after a hydrothermal pre-treatment in aqua regia (5 g L⁻¹) using Ethos Plus computerized

microwave labstation (Milestone General; 50 Hz; heated to 220°C in 8°C increments per minute, kept at 220°C for 15 min, and finally allowed to cool to room temperature). The concentrate consisted mainly of chalcopyrite with pyrite as minor constituent (Figure 5).

Comparison of Fe²⁺-oxidizing abilities of different microbial strains

One-hundred milliliter flasks containing 50 mL HBS medium (pH 2.0; + 0.01% S⁰; + 10 mM Fe²⁺; +TE; ± 0.01% YE) were inoculated with mixed culture containing *At. caldus* KU (1×10⁷ cells mL⁻¹) plus one of the four Fe-oxidizers (*Sb. acidophilus* YTF1, *Sb. sibiricus* N1, *Am. ferrooxidans* ICP or *Acidiplasma* sp. Fv-AP; 1×10⁷ cells mL⁻¹). The flasks were incubated at 45°C, shaken at 150 rpm. Samples were regularly taken for solution analyses (as described below) (water evaporation was compensated with deionized water prior to sampling). All experiments were conducted in duplicate.

Chalcopyrite Bioleaching

Five-hundred milliliter flasks containing 200 mL HBS medium (pH 2.0; + 1% (w v⁻¹) chalcopyrite concentrate; + 0.01% S⁰; + 5 mM Fe²⁺; +TE) were inoculated with mixed culture containing *At. caldus* KU (1×10⁷ cells mL⁻¹) plus one of the four Fe-oxidizers (1×10⁷ cells mL⁻¹). Mixed cultures containing *Am. ferrooxidans* ICP and *Acidiplasma* sp. Fv-AP were prepared with or without 0.01% YE. The flasks were incubated at 45°C,

shaken at 150 rpm. Sterile controls were run in parallel. Samples were regularly taken for solution analyses (as described below) (water evaporation was compensated with deionized water prior to sampling).

Characterization of bioleaching residues over time

Mixed cultures containing *Sb. sibiricus* N1 plus *At. caldus* KU were prepared (as described above) in nine-fold to monitor overtime changes in characteristics of bioleached chalcopyrite concentrate residues. Liquid samples were taken for solution analyses prior to collecting the bioleached residues.

Solution and Solid Analyses

Cell density was monitored by direct counting (Thoma chamber). Liquid samples were first filtered (0.20 μm) to determine concentrations of Fe^{2+} (*o*-phenanthroline method; Caldwell et al. 1946) and total dissolved Fe/Cu (ICP-AES; SEIKO Vista-MPX). E_h values were measured with an Ag/AgCl reference electrode (with an automatic conversion to SHE) (MM-60R, TOADKK).

Solid samples (bioleached residues) were collected by filtration, freeze-dried overnight and analyzed by X-ray diffraction (XRD) (Ultima IV, Rigaku; $\text{CuK}\alpha$ 40 mA, 40 kV), scanning electron microscope (SEM) (JSM-7001F, JEOL), X-ray photoelectron

spectroscopy (XPS) (ESCA 5800, ULVAC-PHI; Al K α) and electron probe micro analyzer (EPMA) (JEOL JXA-8530F; 10 nA, 20 kV).

Results and Discussion

Solution Redox Potentials (E_h) Exhibited by Different Fe-oxidizing Microbes

To screen the conditions for the next bioleaching test, changes in Fe²⁺ concentration, 10 mM initially, and in E_h over time in each mixed culture (*At. caldus* plus one of the four Fe-oxidizers; i.e. *Sb. acidophilus* YTF1, *Sb. sibiricus* N1, *Am. ferrooxidans* ICP or *Acidiplasma* sp. Fv-AP) were determined. The Effect of 0.01% YE on mixotrophic/heterotrophic Fe²⁺ oxidation was also evaluated.

Am. ferrooxidans ICP was the strongest Fe-oxidizer of the group, leading to the quick establishment of higher E_h values (> 800 mV) by day 2. Addition of YE slightly enhanced Fe²⁺ oxidation and cell growth (Figure 1b, c). In the mixed culture with *Sb. sibiricus* N1, YE addition caused a rapid rise in E_h to ~800 mV but did not affect cell density significantly (Fig. 1c). Fe²⁺ oxidation by *Acidiplasma* sp. Fv-AP was slower than that by the former two strains (*Am. ferrooxidans* ICP and *Sb. sibiricus* N1), but it generated higher E_h levels (~800 mV) after day 6 (Fig. 1b). In contrast, a constantly low E_h level (< 600 mV) was maintained in *Sulfobacillus* sp. YTF1 cultures with or without YE addition, due to only minor Fe²⁺ oxidation by the strain (Figure 1a).

Based on the above results, the subsequent bioleaching tests were conducted by selecting the following conditions: i.e., Mixed cultures containing *At. caldus* KU plus one of the following Fe-oxidizers; *Sb. acidophilus* YTF1 (-YE), *Sb. sibiricus* N1 (-YE), *Acidiplasma* sp. Fv-Ap (\pm YE) or *Am. ferrooxidans* ICP (+YE).

Chalcopyrite Bioleaching at Redox Potentials (E_h) Generated by Different Fe-oxidizers

Rapid Fe^{2+} oxidation was observed with *Am. ferrooxidans* ICP and *Acidiplasma* sp. Fv-Ap in the presence of YE (Figure 2d), accompanied by an immediate increase in E_h (>800 and 750 mV, respectively; Figure 2b), and an increase in cell density (up to 7×10^8 cells mL^{-1}), compared to other cultures (Figure 2f). At the same time, less chalcopyrite dissolution was noted with these two strains (Figure 2a, c) than with the others tested. *Am. ferrooxidans* ICP is able to grow autotrophically on Fe^{2+} and heterotrophically on YE (Clark and Norris, 1996). The genus *Acidiplasma* is able to oxidize Fe^{2+} in the presence of trace amount of YE (Golyshina et al. 2009). Therefore, YE promoted strong heterotrophic Fe^{2+} oxidation by the two strains with an immediate rise in E_h . In the absence of YE, a 14-day lag was followed by rapid Fe^{2+} oxidation by *Acidiplasma* sp. Fv-Ap (Fig. 2d), leading to a sudden increase in E_h on day 14 (Fig. 2b). Thus, chalcopyrite dissolution started off rapidly, and then slowed after day 14 (Figure 2a, c), a

clear transition in E_h levels from 550-600 mV to ≥ 700 mV (Figure 2b). With *Sb. sibiricus* N1, Fe^{2+} oxidation became extensive only after day 29 (Figure 2d), creating a clear transition in E_h levels from 550-600 mV to > 700 mV (Figure 2b). Chalcopyrite dissolution readily progressed until the E_h level came to this transition (Figure 2a, c). *Sb. acidophilus* YTF1 showed the weakest Fe^{2+} oxidation throughout (Figure 2d) and E_h values remained stable at around 600 mV (Figure 2b). As a result, dissolution of Cu and Fe progressed continuously for 70 days (Figure 2a, c). Relatively higher pH values (Figure 2e) shown in *Sb. acidophilus* YTF1, *Sb. sibiricus* N1, and *Acidiplasma* sp. Fv-Ap (-YE; only at the beginning) cultures are indicative of greater H^+ -consuming chalcopyrite dissolution that counteracting sulfuric acid production by *At. caldus* KU (Figure 2a, c).

Microscopic observation of morphological differences between *At. caldus* KU (smaller rods) and *Sb. acidophilus* YTF1 cells (larger and longer rods), or between *At. caldus* KU (larger rods) and *Acidiplasma* sp. Fv-Ap cells (smaller irregular cocci) showed that *At. caldus* KU dominated by cell count initially, followed by emergence and gradual increase of respective Fe-oxidizing cells. This observation suggests that autotrophic growth of *At. caldus* KU on S^0 (Hallberg and Lindström, 1994) occurred first, producing cell exudates/lysates of organics that supported subsequent growth of mixotrophic/heterotrophic Fe-oxidizers. Since steady growth of *Sb. sibiricus* N1 is only possible by simultaneous utilization of inorganic substrates (e.g., Fe^{2+} , S^0) and organic

substrates (e.g., yeast extract) (Melamud et al. 2003), sudden initiation of active Fe^{2+} oxidation by *Sb. sibiricus* N1 on day 36 (Figure 2d) was probably the result of accumulation of the organic substrates. Likewise, the heterotrophic Fe^{2+} oxidation by *Acidiplasma* sp. Fv-Ap on day 14 (Figure 2d) was probably the result of release of organics by the autotrophic organisms. Growth of *Sb. acidophilus* YTF1 was reported to occur both autotrophically (on $\text{Fe}^{2+}/\text{S}^0$) and heterotrophically (on yeast extract), although Fe^{2+} oxidation was more rapid and complete in the presence of yeast extract (Norris et al. 1996). Unlike *Sb. sibiricus* N1 and *Acidiplasma* sp. Fv-Ap, weak Fe^{2+} oxidation by *Sb. acidophilus* YTF1 continued steadily. This difference may be due partly to the metabolic inefficiency in utilizing the organic substrates derived from the autotrophs.

The above results indicate that different E_h levels can be created by selected Fe-oxidizers in the bioleaching system. Chalcopyrite dissolution was highly susceptible to the real-time change in E_h and maintaining lower E_h values facilitated a constant Cu solubilization.

Correlation Between Cu Recovery and Normalized Solution Redox Potentials (E_{normal}) During Bioleaching

Until now, only relatively limited studies have examined the effect of controlling E_h of bioleaching systems: Running an electrochemical bioleaching reactor at 600-630 mV

(SHE) resulted in improvement of chalcopyrite leaching when compared to results from conventional bioleaching, chemical leaching and electrochemical leaching. This can be explained by (a) an absence of jarosite formation at the low E_h level, (b) higher cell concentrations achieved by electrochemical Fe^{3+} reduction to Fe^{2+} , and (c) to electro-reduction of chalcopyrite to produce less refractory chalcocite and covellite (Ahmadi et al 2010, 2011). Improved chalcopyrite bioleaching was also observed by controlling E_h at 580 mV (SHE) (Third et al. 2002) or at 620 mV (SHE) (Gericke et al. 2010) through arresting the oxygen supply.

From previous chemical leaching studies, experimental conditions such as metal ion concentrations, solid/liquid ratios and co-existing minerals were shown to affect the optimal E_h value for Cu extraction (Okamoto 2004, 2005; Hiroyoshi 2008a, 2008b). This could cause misleading interpretation of results obtained from different studies conducted under different conditions. In order to define the optimal E_h value independent of such conditional differences, “the normalized redox potential (E_{normal})” was proposed for a reaction model assuming the formation of intermediate Cu_2S from chalcopyrite, with its optimal range being $0 \leq E_{normal} \leq 1$ (highest copper extraction rate achieved at $E_{normal} \approx 0.43$; Okamoto et al. 2004, 2005; Hiroyoshi et al. 2008a, 2008b):

$$E_{normal} = (E_h - E_{ox}) / (E_c - E_{ox}) \quad (5)$$

A reaction model based on E_{normal} has yet to be discussed in detail for bioleaching

studies. We are using the data in Figure 2 of this study to evaluate the effectiveness of the bioleaching reaction based on E_{normal} to reflect real-time concentrations of Fe^{2+} and Cu^{2+} , using equations 3, 4, and 5 in Figure 3.

With *Acidiplasma* sp. Fv-Ap and *Am. ferrooxidans* ICP (+YE), E_{normal} rapidly rose to > 1 ($E > E_c$) due to prompt microbial Fe^{2+} oxidation. The intermediate Cu_2S does not form in this “passive region” (Hiroyoshi et al. 2008a, 2008b). In fact, chalcopyrite leaching was less effective, resulting in only 49 and 48% final Cu recovery, respectively (Figs. 3d and 3e). In *Sb. acidophilus* YTF1 cultures, on the other hand, E_{normal} values were stable within $0 \leq E_{\text{normal}} \leq 1$. The intermediate Cu_2S is formed in this “active region” (Hiroyoshi et al. 2008a, 2008b). In fact, bioleaching under this condition resulted in higher final Cu recovery (75%) (Figure 3a).

Sb. sibiricus N1 and *Acidiplasma* sp. Fv-Ap cultures (-YE) displayed a transition in the E_{normal} level from $0 \leq E_{\text{normal}} \leq 1$ to $E_{\text{normal}} > 1$. This clearly corresponded to the trend of Cu extraction behavior: The E_{normal} values stayed within the optimal range ($0 \leq E_{\text{normal}} \leq 1$) for a longer period in the *Sb. sibiricus* N1 cultures than in the *Acidiplasma* sp. Fv-Ap cultures, resulting in greater Cu recovery in the former (77%) than in the latter (59%) (Fig 2b, c). In sterile controls, copper leaching slowed as E_{normal} approached 0. This was because $E_{\text{normal}} < 0$ ($E_{\text{ox}} > E_h$) indicates a “non-reactive region” (Hiroyoshi et al. 2008a, b) in which Cu_2S is not oxidized and Cu extraction ceases. The final Cu recovery

in sterile controls was 20% (Figure 2f).

Overall, the results suggest that efficiency of chalcopyrite bioleaching can be effectively evaluated by incorporating E_{normal} as a valuation basis which is independent of the real-time change in major metal solutes in the system. The relationship between the Cu leaching rate and E_{normal} is summarized in Figure 4. The maximum Cu leaching rate was achieved at around $E_{\text{normal}} = 0.35$. The optimum E_{normal} value of 0.43, originally reported by Hiroyoshi et al. (2008a, 2008b), was shifted to slightly lower value in this study. This difference may have been caused partly by the higher (45°C) temperature used in this study compared to ambient temperature of 30°C (Hiroyoshi et al. 2008a, 2008b), facilitating the kinetics of chalcocite-intermediate reactions at even lower E_h levels. Another possible explanation is involvement of microbial reactions in this study, compared to abiotic chemical leaching studies (except for one kind of experiment using a mesophilic Fe-oxidizing bacterium) by Hiroyoshi et al. (2008a, b). Thus, (i) Fe-oxidizing microbes generate an Fe-cycle by which they promote chalcocite/covellite oxidation while simultaneously maintaining lower E_{normal} values. (ii) The S^0 , a by product of covellite oxidation, is also solubilized by S^0 -oxidizing cells, which shifts the chemical equilibrium in favor of covellite dissolution. The above microbially mediated covellite dissolution processes (i and ii) may also lower the optimal E_{normal} value slightly in bioleaching compared to chemical leaching.

Changes in Residues During Bioleaching of Chalcopyrite Concentrate with Mixed Cultures Containing *Sb. sibiricus* N1 and *At. caldus* KU

Each flask was incubated until day 2, 7, 12, 21, 26, 31, 38, 55 and 70 to collect all of the bioleached residues remaining in the flask. Cu dissolution and E_{normal} behaviors were reproduced almost identically to results shown in Figure 3b. Thus, the sampling times in this experiment were indicated by overlapping Figure 3b.

According to the XRD results, jarosite and S^0 peaks started to appear at day 38 ($E_{\text{normal}} > \sim 0.6$; Figure 3b), accompanied by distinctive color change of the mineral to yellow (Figure 5). XPS peaks of Cu $2p_{3/2}$ / Cu $2p_{1/2}$ (Figure 6a) and S $2p_{3/2}$ / S $2p_{1/2}$ (Figure 6b) derived from the original chalcopyrite concentrate were observed in bioleached residues until day 31. Sulfate S 2p peaks emerged at day 38. Together with the XRD results, surface-sensitive XPS analyses indicate formation of passivation layers (mostly jarosite) on the chalcopyrite concentrate surface at around day 38, coinciding with declining Cu dissolution after day 38 (Figure 3b).

Hiroyoshi et al. (2004) suggested that oxidation of chalcocite at acidic pHs proceeds according to the following two-step reaction;



Since covellite dissolution is slower than that of chalcocite (Gupta 2003), covellite may be more readily detected during chalcopyrite leaching: In fact, other researchers detected covellite (rather than chalcocite) in bioleached and chemically-leached chalcopyrite residues via Raman spectroscopy (Sasaki et al. 2009) and XRD patterns (Córdoba et al. 2008), respectively. In this study, no direct evidence for intermediate chalcocite or covellite was obtained (by XRD, XAFS, EPMA and XPS; data not shown). Since the original chalcopyrite concentrate contained a minor amount of blue-colored covellite (by EPMA observation; data not shown), it was also not possible to visually confirm the secondary formation of covellite. Detection of such intermediates may become more difficult in active low-redox chalcopyrite bioleaching systems compared to the abiotic counterparts, again because of the effects of microbially mediated covellite dissolution (i and ii), as described in the previous section.

The findings of this study indicate that low Cu leaching rates at higher E_{normal} , especially at $E_{\text{normal}} > 1$ (Fig. 4), were caused by the low reactivity of chalcopyrite at high E_h (Hiroyoshi et al. 2004) and by the passivation mainly due to jarosite that occurred on the chalcopyrite surface.

Kinetics of Bioleaching of Chalcopyrite Concentrate at Different Redox Potentials (E_h)

Mineral dissolution is most frequently interpreted in terms of a shrinking core model.

Such fluid-solid reaction may be generally described as follows:



In this model, the overall reaction proceeds via diffusion through a liquid film (9), diffusion through a product layer (10), and surface chemical reaction (11), one of which steps becomes rate-limiting under certain conditions (Sohn and Wadsworth, 1979):

$$X = k_1 t \quad (9)$$

$$1 - 3(1 - X)^{2/3} + 2(1 - X) = k_d t \quad (10)$$

$$1 - (1 - X)^{1/3} = k_r t \quad (11)$$

Where, X ; the fraction of B reacted, t ; the reaction time, k ; the rate constant

In chalcopyrite dissolution, the fluid film resistance is considered negligible compared to the effects of diffusion through the product layer or of the chemical reactions at the surface. In fact, no linear relationships were obtained between X and t (data not shown). The calculated R^2 and k values are listed in Table II. Data were plotted linearly where R^2 values of regression analyses > 0.97 . Data from day 0 were not plotted to exclude the effect of initial rapid dissolution of covellite, which was a contaminant in the original concentrate.

Surface chemical reaction was likely the rate-limiting step until the end in *Sb. acidophilus* YTF1 cultures (Figure 7a; Table II), where $0 \leq E_{\text{normal}} \leq 1$ was satisfied

throughout the bioleaching period (Figure 3a). A similar trend was found with *Sb. sibiricus* N1 cultures, but only until day 44 (Figure 7a; Table II); this was consistent with $0 \leq E_{\text{normal}} \leq 1$ having being satisfied until day 44 (Figure 3b).

With *Acidiplasma* sp. Fv-Ap (-YE), the initial bioleaching phase (until day 10) appeared to be controlled by a surface chemical reaction, whereas subsequent phases appeared to be controlled by diffusion through the product film (Figure 7b; Table II). This corresponded to the major shift in the E_{normal} level at around day 12 from $0 \leq E_{\text{normal}} \leq 1$ to $E_{\text{normal}} > 1$ (Figure 3b). The E_{normal} level immediately jumped to > 1 in *Acidiplasma* sp. Fv-Ap and *Am. ferrooxidans* ICP cultures (+YE) (Figure 3d and 3e, respectively). In this case, chalcopyrite dissolution was controlled by diffusion through product film throughout the bioleaching period (Figure 7b; Table II). E_{normal} having a value greater than 1 appeared to be consistent with diffusion through product film, resulting from passivation from the precipitation of potassium jarosite ($\text{KFe}_3(\text{OH})_6(\text{SO}_4)_2$) on the surface of the chalcopyrite particles as discussed in the previous section. In sterile controls, the pH values steadily increased owing to the absence of *At. caldus* for production of sulfuric acid (Figure 2e). Ferric precipitation of compounds such as jarosite, detected by XRD analysis (data not shown), resulted therefore in a process consistent with diffusion through product film (Figure 7b).

Different conditions used in previous chemical leaching studies produced

different results suggesting different kinetic mechanism of chalcopyrite leaching. Thus, whereas chemical leaching with non-Fe³⁺ oxidants resulted in dissolution of chalcopyrite controlled by chemical reaction, chemical leaching with Fe³⁺ proceeded through product layer-controlled chalcopyrite dissolution because of passivation of the chalcopyrite surface by jarosite deposition (Dutriziac et al. 1969, 1981). It should be noted that deposition of secondary S⁰ at the chalcopyrite surface did not cause diffusion resistance (Antonić et al. 1994, 2004; Adebayo et al. 2003; Mahajan et al. 2007). However, at fixed pH, *E_h* and temperature, it appears most likely that Fe³⁺ leaching is surface reaction rate-controlled during the initial stage, which is later controlled by surface layer diffusion (Li et al. 2013). Maintaining a lower *E_h* level (e.g., 600-650 mV (SHE)) during chemical chalcopyrite leaching enabled a reaction controlled by surface chemical reaction in ferric sulfate media (Córdoba et al. 2008).

In the case of bioleaching, Fe³⁺ is the essential oxidant in the system. Even though bioleaching is initiated at different *E_h* levels (500-800 mV (SHE)), rapid microbial Fe²⁺ oxidation can increase the *E_h* levels over 800 mV (SHE) within a few days (Córdoba et al. 2008b). Therefore, chalcopyrite bioleaching is highly susceptible to jarosite formation especially at higher pHs (Sasaki et al. 2009; Sandström et al. 2005), leading to the reaction being controlled by diffusion through product film (Pradhan et al. 2010; Abhilash et al. 2013, 2015; Stott et al. 2000).

Consideration of the results of this study and the above-mentioned previous observations leads to the conclusion that the rate-limiting step of chalcopyrite dissolution depends greatly on the E_h value, which fluctuates continually during bioleaching. It was found that efficiency of bioleaching of chalcopyrite could be evaluated on the basis of E_{normal} . Controlling the optimal E_h level (to satisfy $0 \leq E_{normal} \leq 1$; especially at $E_{normal} = \sim 0.35$ at 45°C) in bioleaching systems is thus critical for promoting steady Cu solubilization by a surface chemical reaction. This was possible by selecting a suitable Fe-oxidizing microbe. No physicochemical/electrochemical manipulation was needed.

In actual bioleaching operations, however, a range of indigenous Fe-oxidizing microbes are present on the mineral surface. In order to microbiologically maintain a low E_h level at the mineral surface, prior separate cultivation of mixed cultures containing a “weak” Fe-oxidizer and subsequent inoculation of the ore would be necessary to make it the dominant Fe-oxidizing species in the system. Inclusion of minerals such as PbS that are inhibitory to some microbes (Vilcáez 2015) is a possible means of selectively favoring the growth of weak Fe-oxidizers or of suppressing the activity of indigenous strong Fe-oxidizers. Acidophilic microbes also display different degrees of sensitivity to flotation agents (Okibe and Johnson 2002), which could be exploited in favoring selective growth of preferred Fe-oxidizers in a leaching operation. Further optimization is ongoing to maximize the controlling effect of low redox potential on bioleaching of chalcopyrite

395 concentrate. The utility of the findings of this study is also currently under evaluation

396 using low grade ($< 1\%$) chalcopyrite ores.

397

References

Abhilash GA, Mehta KD, Pandey BD. 2013. Bacterial leaching kinetics for copper dissolution from a low-grade Indian chalcopyrite ore. *Rem: Rev Esc Minas* 66:245-250.

Abhilash GA, Pandey BD. 2015. Bioleaching of low grade granitic chalcopyrite ore by hyperthermophiles: Elucidation of kinetics-mechanism. *Metall Res Technol* 112:506.

Adebayo AO, Ipinmoroti KO, Ajayi OO. 2003. Dissolution kinetics of chalcopyrite with hydrogen peroxide in sulphuric acid medium. *Chem Biochem Eng Q* 17:213-218.

Ahmadi A, Schaffie M, Manafi Z, Ranjbar M. 2010. Electrochemical bioleaching of high grade chalcopyrite flotation concentrates in a stirred bioreactor. *Hydrometallurgy* 104:99-105.

Ahmadi A, Schaffie M, Petersen J, Schippers A, Ranjbar M. 2011. Conventional and electrochemical bioleaching of chalcopyrite concentrates by moderately thermophilic bacteria at high pulp density. *Hydrometallurgy* 106:84-92.

Antonijević MM, Janković Z, Dimitrijević M. 1994. Investigation of the kinetics of

417 chalcopyrite oxidation by potassium dichromate. Hydrometallurgy 35:187-201.

418

419 Antonijević MM, Janković ZD, Dimitrijević MD. 2004. Kinetics of chalcopyrite

420 dissolution by hydrogen peroxide in sulphuric acid. Hydrometallurgy 71:329-334.

421

422 Boeckstein A, Stadhouders AM, Stols ALH, Roomans GM. 1983. A comparison of

423 ZAF-correction methods in quantitative X-ray microanalysis of light-element specimens.

424 Ultramicroscopy 12:65-68.

425

426 Caldwell DH, Adams RB. 1946. Colorimetric determination of iron in water with

427 *o*-phenanthroline. J Am Water Works Ass 38:727-730.

428

429 Clark DA, Norris PR. 1996. *Acidimicrobium ferrooxidans* gen. nov., sp. nov.:

430 mixed-culture ferrous iron oxidation with *Sulfobacillus* species. Microbiology

431 142:785-790.

432

433 Córdoba EM, Muñoz JA, Blázquez ML, González F, Ballester A. 2009. Passivation of

434 chalcopyrite during its chemical leaching with ferric ion at 68°C. Miner Eng 22:229-235.

435

Córdoba EM, Muñoz JA, Blázquez ML, González F, Ballester A. 2008a. Leaching of chalcopyrite with ferric ion. Part II: Effect of redox potential. *Hydrometallurgy* 93:88-96.

Córdoba EM, Muñoz JA, Blázquez ML, González F, Ballester A. 2008b. Leaching of chalcopyrite with ferric ion. Part IV: The role of redox potential in the presence of mesophilic and thermophilic bacteria. *Hydrometallurgy* 93:106-115.

Dutrizac JE. 1981. The dissolution of chalcopyrite in ferric sulphate and ferric chloride media. *Metall Trans B* 12B:371-378.

Dutrizac JE, MacDonald JC, Ingraham TR. 1969. The kinetics of dissolution of synthetic chalcopyrite in aqueous acidic ferric sulphate solution. *T Metall Soc Aime* 245:955-959.

Gericke M, Govender Y, Pinches A. 2010. Tank bioleaching of low-grade chalcopyrite concentrates using redox control. *Hydrometallurgy* 104:414-419.

Ghahremaninezhad A, Dixon DG, Asselin E. 2013. Electrochemical and XPS analysis of chalcopyrite (CuFeS_2) dissolution in sulfuric acid solution. *Electrochim Acta* 87:97-112.

Golyshina OV, Yakimov MM, Lünsdorf H, Ferrer M, Nimtz M, Timmis KN, Wray V, Tindall BJ, Golyshin PN. 2009. *Acidiplasma aeolicum* gen. nov., sp. nov., a euryarchaeon of the family *Ferroplasmaceae* isolated from a hydrothermal pool, and transfer of *Ferroplasma cupricumulans* to *Acidiplasma cupricumulans* comb. nov. Int J Syst Evol Microbiol 59:2815-2823.

Gupta CK. 2003. Chemical Metallurgy: Principles and Practice. Weinheim: Wiley-VCH Verlag GmbH & Co. KGaA. 842p.

Hallberg KB, Lindström EB. 1994. Characterization of *Thiobacillus caldus* sp. nov., a moderately thermophilic acidophile. Microbiology 140:3451-3456.

Hiroyoshi N, Kitagawa H, Tsunekawa M. 2008a. Effect of solution composition on the optimum redox potential for chalcopyrite leaching in sulfuric acid solutions. Hydrometallurgy 91:144-149.

Hiroyoshi N, Kuroiwa S, Miki H, Tsunekawa M, Hirajima T. 2004. Synergistic effect of cupric and ferrous ions on active-passive behavior in anodic dissolution of chalcopyrite in sulfuric acid solutions. Hydrometallurgy 74:103-116.

Hiroyoshi N, Miki H, Hirajima T, Tsunekawa M. 2000. A model for ferrous-promoted chalcopyrite leaching. *Hydrometallurgy* 57:31-38.

Hiroyoshi N, Miki H, Hirajima T, Tsunekawa M. 2001. Enhancement of chalcopyrite leaching by ferrous ions in acidic ferric sulfate solutions. *Hydrometallurgy* 60:185-197.

Hiroyoshi N, Tsunekawa M, Okamoto H, Nakayama R, Kuroiwa S. 2008b. Improved chalcopyrite leaching through optimization of redox potential. *Can Metall Quart* 47:253-258.

Klauber C, Parker A, Bronswijk W, Watling H. 2001. Sulphur speciation of leached chalcopyrite surfaces as determined by X-ray photoelectron spectroscopy. *Int J Miner Process* 62:65-94.

Li Y, Kawashima N, Li J, Chandra AP, Gerson AR. 2013. A review of the structure, and fundamental mechanisms and kinetics of the leaching of chalcopyrite. *Adv Colloid Interface Sci* 197-198:1-32.

493 Mahajan V, Misra M, Zhong K, Fuerstenau MC. 2007. Enhanced leaching of copper
 494 from chalcopyrite in hydrogen peroxide–glycol system. *Miner Eng* 20:670-674.
 495
 496 Masaki Y, Hirajima T, Sasaki K, Okibe N. 2015. Bioreduction and immobilization of
 497 hexavalent chromium by the extremely acidophilic Fe(III)□reducing bacterium
 498 *Acidocella aromatica* strain PFBC. *Extremophiles* 19:495-503.
 499
 500 Masaki Y, Tsutsumi K, Hirano S, Okibe N. 2016. Microbial community profiling of
 501 Chinoike Jigoku (“Blood Pond Hell”) hot spring in Beppu, Japan and isolation and
 502 characterization of Fe(III)-reducing *Sulfolobus* sp. strain GA1. *Res Microbiol*
 503 167:595-603.
 504
 505 Melamud VS, Pivovarova TA, Tourova TP, Kolganova TV, Osipov GA, Lysenko AM,
 506 Kondrat’eva TF, Karavaiko GI. 2003. *Sulfobacillus sibiricus* sp. nov., a new moderately
 507 thermophilic bacterium. *Microbiology* 72:605-612.
 508
 509 Norris PR, Clark DA, Owen JP, Waterhouse S. 1996. Characteristics of *Sulfobacillus*
 510 *acidophilus* sp. nov. and other moderately thermophilic mineral-sulphide-oxidizing
 511 bacteria. *Microbiology* 142:775-783.

512

513 Okamoto H, Nakayama R, Hiroyoshi N, Tsunekawa M. 2004. Redox potential
514 dependence and optimum potential of chalcopyrite leaching in sulfuric acid solutions.
515 Journal of MMIJ 120:592-599 (in Japanese).

516

517 Okamoto H, Nakayama R, Kuroiwa S, Hiroyoshi N, Tsunekawa M. 2005. Normalized
518 redox potential used to assess chalcopyrite column leaching. Journal of MMIJ
519 121:246-254 (in Japanese).

520

521 Okibe N, Johnson DB. 2002. Toxicity of flotation reagents to moderately thermophilic
522 bioleaching microorganisms. Biotechnol Lett 24:2011-2016.

523

524 Parker AJ, Paul RL, Power GP. 1981. Electrochemistry of the oxidative leaching of
525 copper from chalcopyrite. J Electroanal Chem 118:305-316.

526

527 Pradhan D, Kim DJ, Chaudhury GR, Sohn JS, Lee SW. 2010. Dissolution kinetics of
528 complex sulfides using acidophilic microorganisms. Mater Trans 51:413-419.

529

530 Sandström □, Shchukarev A, Paul J. 2005. XPS characterisation of chalcopyrite

chemically and bio-leached at high and low redox potential. Miner Eng 18:505-515.

Sasaki K, Nakamuta Y, Hirajima T, Tuovinen OH. 2009. Raman characterization of secondary minerals formed during chalcopyrite leaching with *Acidithiobacillus ferrooxidans*. Hydrometallurgy 95:153-158.

Sillitoe RH. 2010. Porphyry copper systems. Econ Geol 105:3-41.

Sohn HY. 1979. Fundamentals of the kinetics of heterogeneous reaction systems in extractive metallurgy. In: Sohn HY, Wadsworth ME, editors. Rate Processes of Extractive Metallurgy. New York: Springer. P 1-51.

Stott MB, Watling HR, Franzmann PD, Sutton D. 2000. The role of iron-hydroxy precipitates in the passivation of chalcopyrite during bioleaching. Miner Eng 13:1117-1127.

Third KA, Cord-Ruwisch R, Watling HR. 2002. Control of the redox potential by oxygen limitation improves bacterial leaching of chalcopyrite. Biotechnol Bioeng 78:433-441.

550 Vilcáez J. 2015. On the mechanism of chalcopyrite bioleaching with thermophiles. Aust J
551 Earth Sci 2:1-4.

552

553 Viramontes-Gamboa G, Peña-Gomar MM, Dixon DG. 2010. Electrochemical hysteresis
554 and bistability in chalcopyrite passivation. Hydrometallurgy 105:140-147.

555

556 Viramontes-Gamboa G, Rivera-Vasquez BF, Dixon DG. 2007. The active-passive
557 behavior of chalcopyrite. J Electrochem Soc 154:299-311.

Figure Legends

Figure 1.

Changes in Fe^{2+} concentrations (a) and redox potentials (E_h) (b) during growth (c) of each of four different Fe-oxidizers (*Sb. acidophilus* YTF1 (●, ○) / *Sb. sibiricus* N1 (■, □) / *Acidiplasma* sp. Fv-Ap (▲, △) / *Am. ferrooxidans* ICP (◆, ◇)) in mixed culture with *At. caldus* KU. Sterile controls (+, ×) were run in parallel. Cell densities in the samples were determined by counting the cells of *At. caldus* KU and the other Fe-oxidizer with which it was combined. Solid lines indicate addition of 0.01% yeast extract. Broken lines indicate no yeast extract addition. Data points are mean values from duplicate cultures. Error bars depicting averages are not visible in some cases as these were smaller than the data point symbols.

Figure 2.

Changes in total soluble Cu concentrations (a), E_h values (b), total soluble Fe concentrations (c), Fe^{2+} concentrations (d), pH values (e) and cell densities (f) during bioleaching of chalcopyrite concentrate. Mixed cultures contained *At. caldus* KU plus one of the following Fe-oxidizers: *Sb. acidophilus* YTF1 (●) / *Sb. sibiricus* N1 (■) / *Acidiplasma* sp. Fv-Ap (▲) / *Acidiplasma* sp. Fv-Ap (+YE) (▼) / *Am. ferrooxidans* ICP (+YE) (◆). Sterile controls (×) were run in parallel. Cell densities represented the total

of all bacterial cells in a sample. Data points are mean values from duplicate cultures.

Error bars depicting averages are not visible in some cases as these were smaller than the data point symbols. “+YE” indicates addition of 0.01% yeast extract.

Figure 3.

Relationship between the normalized redox potential (E_{normal} ; open symbols) and dissolution of Cu (solid symbols on solid lines) and Fe (solid symbols on broken lines) during bioleaching of chalcopyrite concentrate. Each of four Fe-oxidizing microbes

(inoculated at 1×10^7 cells mL^{-1}) was used in mixed cultures with S-oxidizing *At. caldus*

KU (inoculated at 1×10^7 cells mL^{-1}): (a) *Sb. acidophilus* YTF1; (b) *Sb. sibiricus* N1; (c)

Acidiplasma sp. Fv-Ap; (d) *Acidiplasma* sp. Fv-Ap (+YE); (e) *Am. ferrooxidans* ICP

(+YE). Sterile controls (f) were run in parallel. “+YE” stands for addition of 0.01% yeast

extract in the media. Data points are mean values from duplicate cultures. Error bars

depicting averages are not visible in some cases as these were smaller than the data point

symbols.

Figure 4.

Relationship between the Cu leaching rate and the E_{normal} value. The plots originated from

mixed culture containing *At. caldus* KU plus one of the following Fe-oxidizers; *Sb.*

acidophilus YTF1 (●) / *Sb. sibiricus* N1 (■) / *Acidiplasma* sp. Fv-Ap (▲) /
Acidiplasma sp. Fv-Ap (+YE) (▼) / *Am. ferrooxidans* ICP (+YE) (◆). Sterile controls
(×) were also included. A single triangle plot (▲) positioned at exceptionally high Cu
leaching rate of 2.2, likely resulted from rapid oxidation of chalcocite/covellite
(accumulated before day 14) triggered by a jump in the E_{normal} level at day 14 (Figure 3c).

Figure 5.

X-ray diffraction patterns and the color change of original chalcopyrite concentrate and
bioleached residues in mixed cultures containing *At. caldus* KU plus *Sb. sibiricus* N1
collected on day 2, 7, 12, 21, 26, 31, 38, 55, or 70. C; chalcopyrite (ICSD 2518), P; pyrite
(ICSD 633289), J; potassium jarosite (ICSD 166801), S; elemental sulfur (ICSD
412326).

Figure 6.

XPS spectra of Cu 2p (a) and S 2p (b) of chalcopyrite concentrates bioleached in mixed
cultures containing *Sb. sibiricus* N1 and *At. caldus* KU. Samples were collected at day 2,
7, 12, 21, 26, 31, 38, and 55. Peak positions corresponding to original chalcopyrite (Cu
2p_{3/2} = 932.4 eV, Cu 2p_{1/2} = 952.3 eV, S 2p_{3/2} = 161.4 eV, S 2p_{1/2} = 162.5 eV;
Ghahremaninezhad et al. 2013) are indicated by vertical grey bars. Peak positions

corresponding to sulfate (S 2p_{3/2} = 168.7 eV, S 2p_{1/2} = 169.9 eV; Klauber et al. 2001) are indicated by grey broken lines. The doublet S 2p peaks (161.4 eV and 162.5 eV) reflect the occurrence of monosulfide and disulfide (Ghahremaninezhad et al. 2013). The shift (to higher binding energies) of Cu 2p_{3/2} and Cu 2p_{1/2} peaks originating from chalcopyrite was likely the result of a differential charging effect.

Figure 7.

Kinetic modeling of chalcopyrite bioleaching in mixed cultures containing *At. caldus* KU plus the following Fe-oxidizers; *Sb. acidophilus* YTF1 (●) / *Sb. sibiricus* N1 (■) / *Acidiplasma* sp. Fv-Ap (▲) / *Acidiplasma* sp. Fv-Ap (+YE) (▼) / *Am. ferrooxidans* ICP (+YE) (◆). Sterile controls (×) are also included. The rate-limiting step was assumed to be (a) surface chemical reaction or (b) diffusion through product film. Linear lines were drawn where R² values were calculated to be > 0.97. Day 0 plots were excluded to remove the effect of initial rapid dissolution of covellite contaminating the original chalcopyrite concentrate.

Table 1.

Elemental composition of chalcopyrite concentrate used in this study.

634 **Table 2.**

635 R^2 and k values calculated using the kinetic model of surface chemical reaction and
636 diffusion through product film.

637 **Acknowledgement**

638 Chalcopyrite concentrate was kindly provided by JX Nippon Mining & Metals. *Sb.*
639 *acidophilus* strain YTF1 and *Acidiplasma* sp. strain Fv-Ap were kindly provided by Prof.
640 D.B. Johnson (Bangor University, UK). The XAFS experiments were performed at
641 Kyushu University Beamline (Saga-LS /BL06) with the proposal No. of 2016IK003 and
642 2016IHK013. We would like to thank Mr. Kazuhiko Shimada (Department of Earth and
643 Planetary Sciences, Kyushu University) for his technical support with the EPMA analysis.
644 Y.M. is thankful for financial assistance provided by the Kyushu University Advanced
645 Graduate Program in Global Strategy for Green Asia.